JOURNAL OF MATERIALS SCIENCE 29 (1994) 4771–4777

Microstructure and growth of electrodeposited nanocrystalline nickel foils

Á. CZIRÁKI, B. FOGARASSY, I. GERÖCS
Institute for Solid State Physics, Eötvös University, Múzeum krt. 6-8, H-1088 Budapest, Hungary

E. TÓTH-KÁDÁR, I. BAKONYI
Research Institute for Solid State Physics, Hungarian Academy of Sciences, P.O.B. 49, H-1525 Budapest, Hungary

In the present work, the structure of electrodeposited pure Ni foils has been investigated by X-ray diffractometry, transmission electron microscopy and by measuring their electrical transport properties. It was found that the as-deposited Ni foils have a nanocrystalline structure covered by a thin amorphous Ni layer on the substrate side: the growth of the electrodeposited foils starts in amorphous form followed by nanocrystalline layers. To explain the formation of the amorphous Ni layer, it is supposed that foreign atoms are incorporated into the nucleating Ni films.

1. Introduction

Nanocrystalline materials have recently received considerable attention as a result of their unique physical, chemical and mechanical properties [1]. In polycrystalline materials with nanometre-sized grains, a substantial fraction of atoms belongs to the crystalline interfaces and this fact, usually, has a profound influence on the physical properties. This new class of disordered solids introduces such a high density of defect cores that 50% or more of the atoms can be situated in the cores of these defects. Depending on the types of defect involved, nanocrystalline materials with different structures may be generated. For example, the atomic structures of the core regions of the various boundaries between the crystallites may differ because their structure depends on the crystal misorientations and boundary inclinations. The boundary core regions are characterized [2] by a reduced atomic density and an increased average interatomic spacing deviating from the ones in the perfect lattice. Estimates from small-angle X-ray and neutron diffraction experiments [3,4] have, indeed, indicated that the grain boundaries in nanocrystalline materials have a remarkably low density for a solid-state structure, much lower than the density of glasses which, usually, deviates from the crystalline density by a few per cent only.

As far as the atomic structure of the interfacial component in nanocrystalline metals is concerned, the situation is still rather controversial. Gleiter and co-workers [3–6] deduced from their experiments that these grain boundaries possess neither long-range nor short-range order. On the other hand, the results of Eastman and co-workers [7–10] led to the conclusion that there is no evidence for the presence of extended, disordered boundary regions in nanocrystalline metals that would differ from boundaries in coarse-grained materials.

Anyway, recent developments in the synthesis of these materials have stimulated interest in protective and functional coating applications. Electrodeposition has been found to be a convenient method for the preparation of nanocrystalline metals; it is technically simple and generally inexpensive. Electrodeposition of pure Ni under suitable conditions leads to nanocrystalline structures [11–14].

In this paper we present X-ray diffraction (XRD) and transmission electron microscopy (TEM) investigations of the microstructure of electrodeposited (ED) nanocrystalline pure Ni foils and discuss the effect of the fine-grained structure on some physical properties and, especially, on the growth characteristics of the crystallites during deposition.

2. Experimental procedure

For the present studies, nickel electrodeposits were prepared at different deposition current densities with direct-current electroplating by using a flowing electrolyte system [15]. ED Ni foils in the form of circular discs of diameter 70 mm were produced in this way from a plating bath [16] containing $NiSO_4$, Na_2SO_4 and HCOOH on to 30 μm thick polished polycrystalline Cu foils which were then dissolved from the Ni deposit. Only the central 50 mm diameter part cut out of the discs was used for further studies in the as-deposited state. Two parallel series of samples denoted by TD1 and TD2 have been produced under nominally identical conditions with foil thicknesses ranging from 4 to 22 μm. The results of a mass spectrometric analysis of one of the samples prepared with $i_{dep} = 100$ mA cm^{-2} indicated [14] that the total amount

0022–2461

of impurities was very small (about 0.44 wt % with Co (0.28 wt %) as the main impurity) in these ED Ni foils.

The resistivity (ρ) of the samples was determined by a d.c. four-point technique with the help of a fixed arrangement of gold-plated pins placed on the Ni disc and calibrating the geometrical constant of the arrangement on a Cu foil. The resistance R was measured at 300 and 77 K (in the latter case by immersing the probe with the mounted sample into liquid nitrogen) and the temperature coefficient of resistivity was obtained as $\alpha = (R_{300\,K} - R_{77\,K})/R_{300\,K}(300 - 77)$. An advantage of studying α is that it is a geometry-independent quantity and can be measured to an accuracy of a few per cent.

The structure of the deposits was studied by TEM and by XRD.TEM studies were performed using a Jeol 100C transmission electron microscope. Thin foils for TEM studies were prepared by jet-polishing using a 70% ethanol and 30% perchloric acid solution at − 40° C. However, since the deposits often contained small pinholes, in their vicinity a TEM study could be performed even without a thinning procedure.

From the XRD line-broadening of the (1 1 1) and (2 0 0) lines of *f.c.c.* Ni, the apparent crystallite size L was determined using the equation $L = \lambda/(\beta\cos\theta)$ where λ is the X-ray wavelength (CuK_α in our case), θ the Bragg angle and β the line-broadening. The quantity β was determined from the expression $\beta^2 = \beta^2_{meas} - \beta^2_{inst}$ where β_{inst} is the instrumental half-maximum full width measured on the peaks of a coarse-grained sample and β_{meas} is the half-maximum full width of the investigated nanocrystalline sample (β is measured in *radians*). Since the crystallite size obtained in this manner was in good agreement with the directly determined grain sizes via TEM observations, it is believed that the contribution of internal stresses to the XRD line-broadening was negligible in our samples.

3. Results and discussion

3.1 Electrical transport properties

The magnitude of the room-temperature resistivity $\rho_{300\,K}$ and the temperature coefficient of resistivity α are shown in Fig. 1a and b, respectively, as a function of the deposition current density i_{dep}. It can be seen that the resistivity is higher for all samples than the corresponding value for *f.c.c.* μc-Ni [17]. The notation μc is used here, by analogy with *nc* for nanocrystalline, to denote a microcrystalline state, *i.e.* the state when the grain size is in the micrometre range as is the case for the well-annealed Ni samples studied by Laubitz *et al.* [17]. Although $\rho_{300\,K}$ has a relatively large error (about ± 1 μΩ cm) due to the approximately 10% uncertainty of the thickness determination, there is a clear tendency that $\rho_{300\,K}$ increases with decreasing deposition current density. By using the resistivity increment values due to dissolved impurities in Ni, for both substitutional [18] and interstitial [19] impurities, it can be estimated from the results of mass

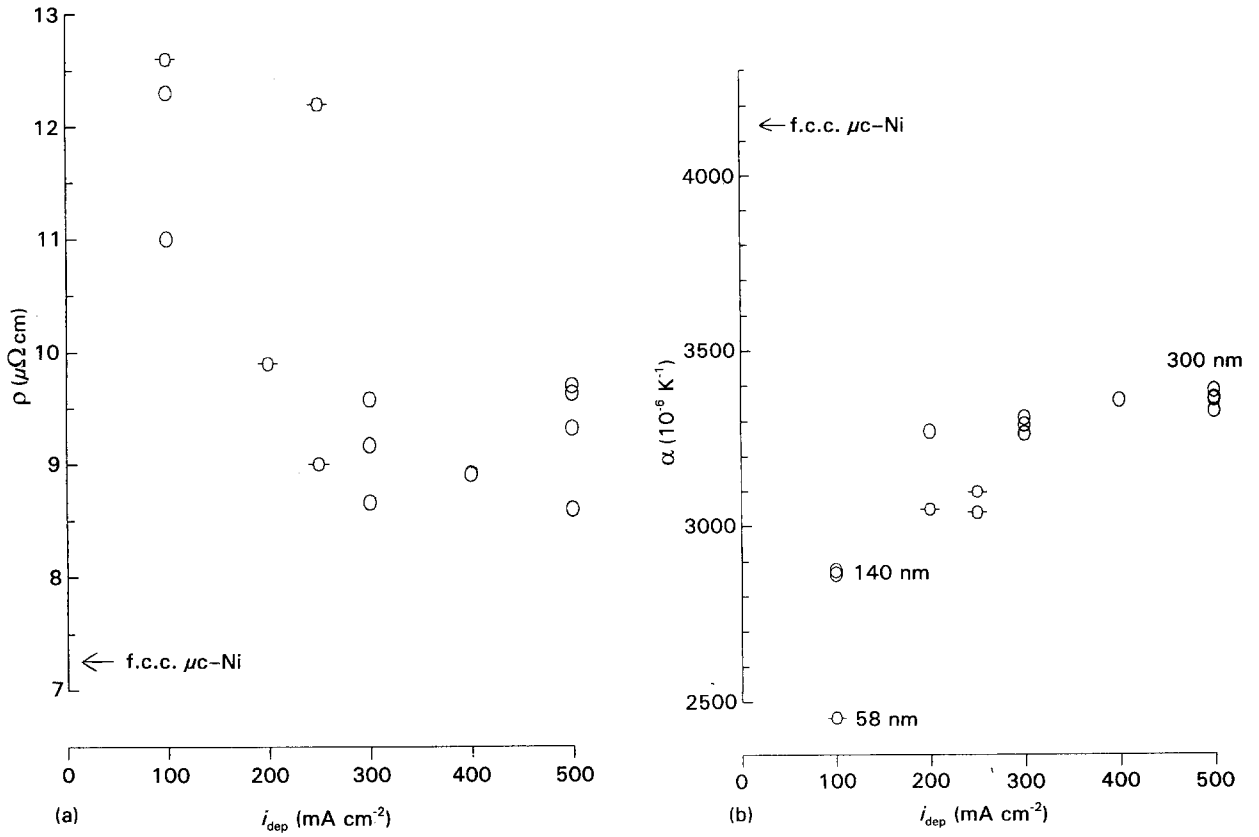

Figure 1 (a) Room-temperature electrical resistivity $\rho_{300\,K}$ and (b) temperature coefficient of resistivity α versus deposition current density i_{dep} for ED Ni foils: (○) TD1, (-o-) TD_2. The numbers attached to some data point symbols represent the average grain size determined for that sample by XRD and/or by TEM. For the samples with $i_{dep} = 100$ mA cm^{-2} in (b), the thickness was 4 and 7 μm for the lower and higher α value, respectively. The arrows on the ordinate indicate the values for *f.c.c.* μc-Ni from Laubitz *et al.* [17]. Errors (a) ± 1 μΩ cm, (b) ± 100 × 10^{-6} K^{-1}.

spectrometry analysis [14] that the resistivity increase due to impurities in our ED Ni samples can amount to about 1 to 1.5 μΩ cm) with respect to *f.c.c.* μc-Ni. Fig. 1a shows that the samples prepared with high values of i_{dep} have $\rho_{300\,K}$ values which are higher by about this amount than the value for coarse-grained Ni. The resistivity of samples for smaller values of i_{dep} is significantly higher, which is ascribed [14] to the nanocrystalline character of these ED Ni foils. Namely, if the grain size becomes sufficiently small, the volume fraction of grain boundaries which have strong topological disorder will no longer be negligible, and this is expected to lead to a well-measurable increase of the resistivity.

On the other hand, it is well known [20] that for disordered metals an increase of the resistivity is generally accompanied by a decrease of its temperature coefficient α. As Fig. 1b shows, this is the case for the present ED Ni samples as well: the higher is $\rho_{300\,K}$, the smaller is α and, also, all the α values are well below that of *f.c.c.* μc-Ni. These facts strongly support the interpretation that the deviation of electrical transport properties from the corresponding parameters of coarse-grained Ni can be ascribed to a higher degree of topological disorder in the ED Ni samples. As will be revealed by the diffraction studies described below, this increased disorder is due to the fine-grained structure of our Ni electrodeposits.

It should still be noted that, in most cases, the two series of samples gave fairly identical results for $\rho_{300\,K}$ and α. Also, there was no significant dependence on foil thickness in the range investigated except for the samples prepared with the smallest deposition current density (Fig. 1b, $i_{dep} = 100$ mA cm^{-2}) where also the grain size was the smallest. Since in this latter case the only difference between the samples was their thickness, special attention was paid here to establishing the grain sizes of both kind of samples.

TABLE I Grain size determined by XRD and TEM as a function of the deposition current density i_{dep} and the thickness of the ED Ni samples (in cases where grain size values from both XRD and TEM investigations are included, they were obtained on the same disc samples)

Thickness (μm)	Average grain size (nm)							
	100 mA cm^{-2}		200 mA cm^{-2}		250 mA cm^{-2}		500 mA cm^{-2}	
	XRD	TEM	XRD	TEM	XRD	TEM	XRD	TEM
4–5	55 ± 5	60 ± 10			62 ± 5		> 200	300 ± 50
7–9	130 ± 10	150 ± 20		250 ± 50	> 200			

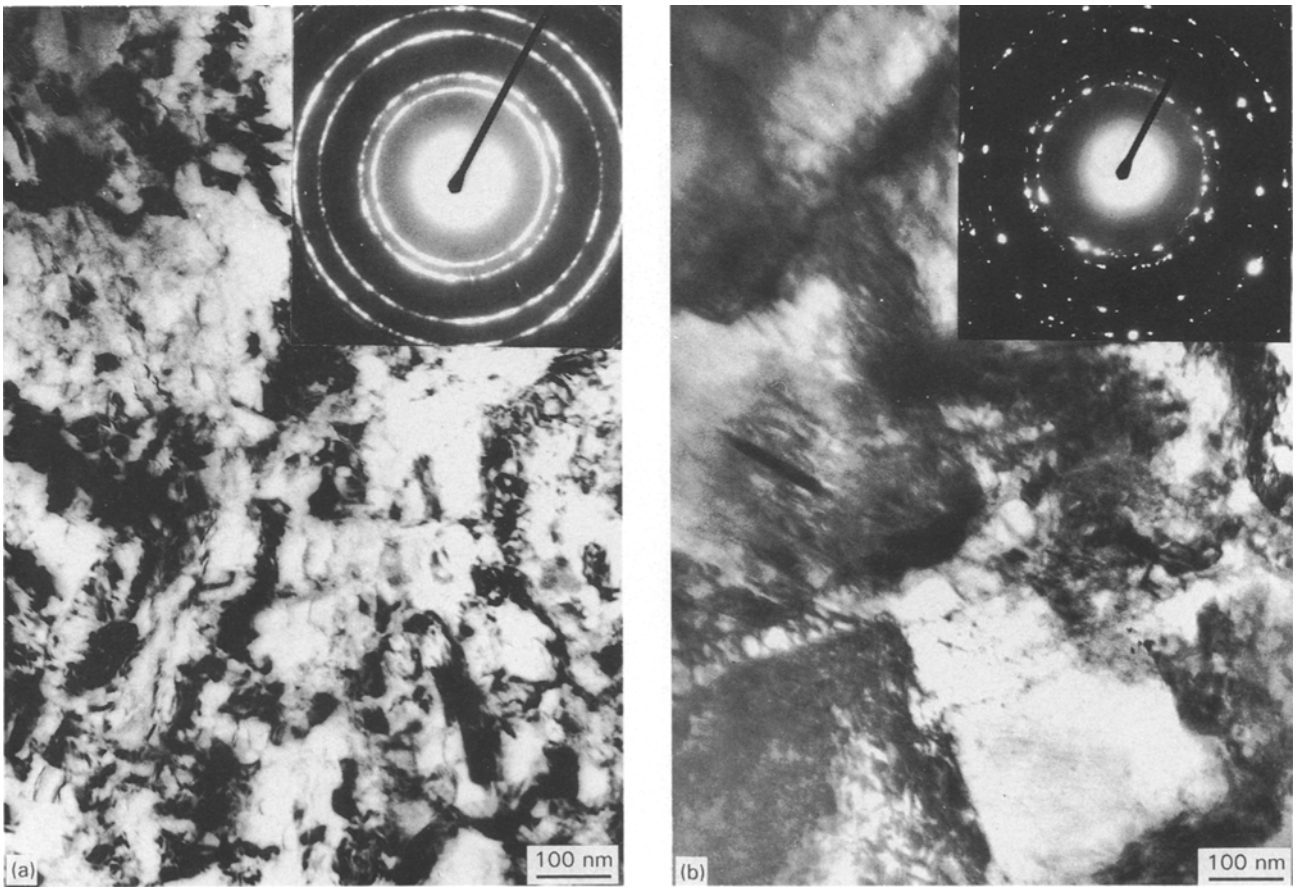

Figure 2 TEM picture and the corresponding selected-area diffraction pattern of ED Ni foils prepared with $i_{dep} = 100$ mA cm^{-2} and having a thickness of (a) 4 μm and (b) 7 μm.

Figure 3 TEM picture of a different area of the same sample as in Fig. 2a, shown at a higher magnification.

3.2. Microstructure

The results of grain size determinations are summarized in Table I. As far as the data from XRD are concerned, they were obtained by averaging effective grain size values for the two reflections investigated (the (1 1 1) and (2 0 0) lines). The intensity ratio I_{200}/I_{111} was 2.7 for the sample with the smallest grain size and about 5.5 for all the other samples studied by XRD, whereas this ratio is 0.42 for coarse-grained *f.c.c.* Ni. This indicates a strongly preferred texture of the ED Ni foils, specifically with the (1 0 0) planes oriented predominantly along the foil surface. The XRD and TEM investigations indicated that, in general, the average size of the crystallites is smaller in the thinner samples.

Typical electron microscopic pictures and corresponding selected-area diffraction patterns of samples deposited with $i_{dep} = 100\ mA\ cm^{-2}$ are shown in Fig. 2 for two different foil thicknesses. The sample of foil thickness 4 μm (Fig. 2a) consists of nanometre-sized crystallites with an average diameter of about 60 nm. As can be seen from the high-magnification picture (Fig. 3) of the same sample, a large number of grains have a very small size, as low as 5–6 nm, in the thinner sample deposited with $100\ mA\ cm^{-2}$. On the other hand, the sample prepared also with $i_{dep} = 100\ mA\ cm^{-2}$ and having a thickness of 7 μm has a grain size of about 150 nm (Fig. 2b). It should furthermore be noted that the selected-area diffraction patterns of these two samples further support the grain size differences shown by the electron micrographs.

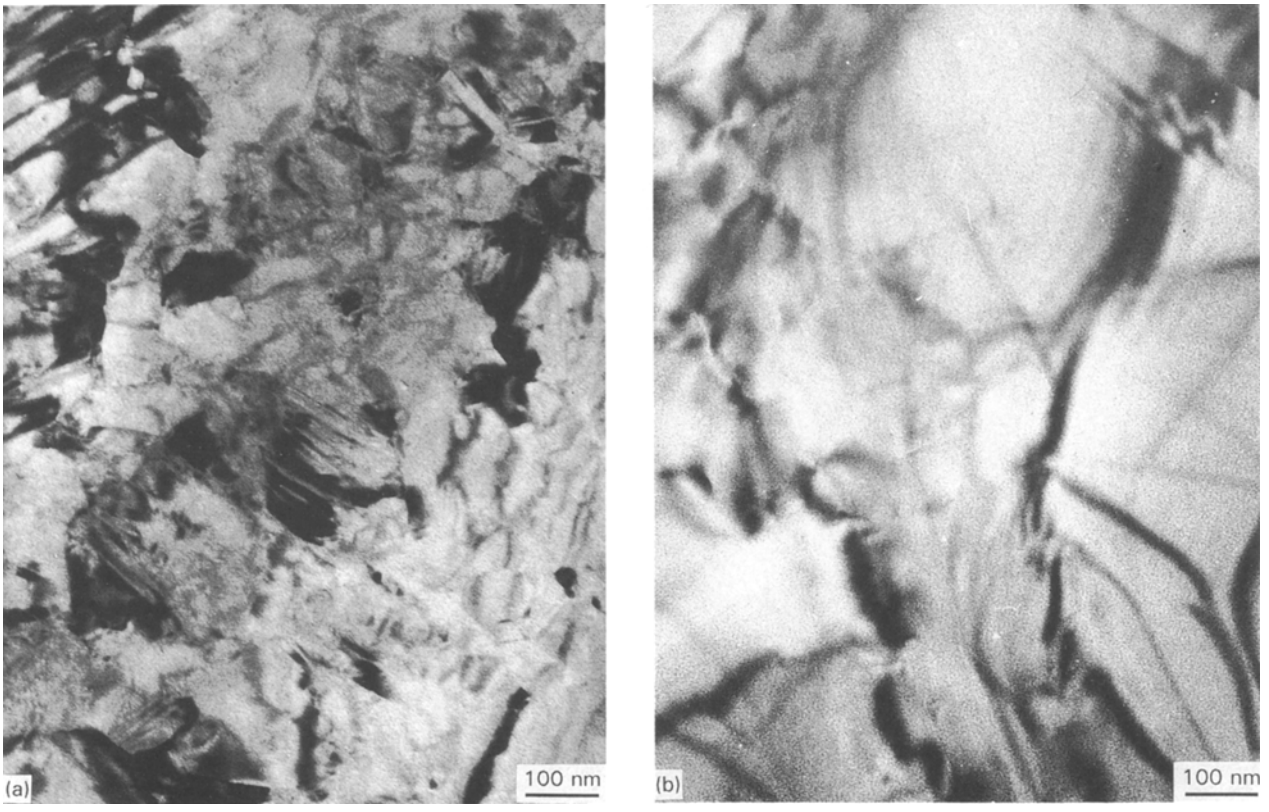

Figure 4 TEM pictures of ED Ni foils having thicknesses of about 4 to 5 μm and prepared with (a) $i_{dep} = 100\ mA\ cm^{-2}$ (a different area of the same sample to that in Fig. 2a) and (b) $i_{dep} = 500\ mA\ cm^{-2}$.

These observations are in good agreement with the lower value of the temperature coefficient of resistivity for the thinner sample (Fig. 1b) which indicates increasing structural disorder as a result of an increasing volume fraction of grain boundaries.

Comparing samples having approximately the same thickness, it was established that the average grain size of the samples prepared with higher current density is higher (Table I). A typical series of electron microscopic pictures demonstrating these features is shown in Fig. 4. The observed variation of the grain size with i_{dep} strongly supports the interpretation described in section 3.1, according to which the variation of the electrical transport properties was ascribed to structural disorder due to the large amount of grain boundaries.

The feature that α was not found to be sensitive to the foil thickness for higher values of i_{dep} (for $\rho_{300\,K}$, the large relative error masks such a dependence even at $i_{dep} = 100$ mA cm^{-2}) can originate in the fact that a coarser-grained layer on one side of the foil acts as a low-resistivity shunt and this side predominantly determines the behaviour of the electrical transport parameters and, therefore, this phenomenon will be investigated in some detail below.

3.3. Growth process during deposition

The fact, found in some cases from TEM and electrical resistivity measurements, that the deposited pure Ni layers produced under nominally identical conditions are still different in microstructure depending on their thickness indicates the possibility of a gradual coarsening of the deposit during the layer growth process.

To prove this interpretation of the above observed effect, the regions surrounding pinholes have been studied by TEM. Due to the shape of the edge, these places of the deposited layers are very advantageous for studying the growth process. As mentioned before, the samples have some pinholes in the as-made state without any further special thinning. This is a very important and lucky fact because there is no danger of artefacts due to the sample preparation process.

Around these natural holes, very interesting amorphous areas have been detected by selected-area electron diffraction (Fig. 5). In the neighbourhood of these amorphous regions an extra fine-grained structure was found with an average grain diameter of 5–6 nm (Fig. 6), even in the case of a sample deposited with a current density of 500 mA cm^{-2}. It is noted that this sample has a relatively large average grain size of about 300 nm as a bulk material (Table I). Approaching from the edge of the hole to the inner part of the deposit, the very fine-grained and coarser-grained layers lie on each other according to the selected-area diffraction pattern (see the very fine-grained polycrystalline rings with single-crystal diffraction superimposed on them in Fig. 7). The very thin amorphous layer is presumed to be present on the bottom of the deposited layer, as was found at the hole, but its diffuse ring is not visible any more due to the strong diffraction patterns of the thick nanocrystalline layers. This assumption is supported by the fact

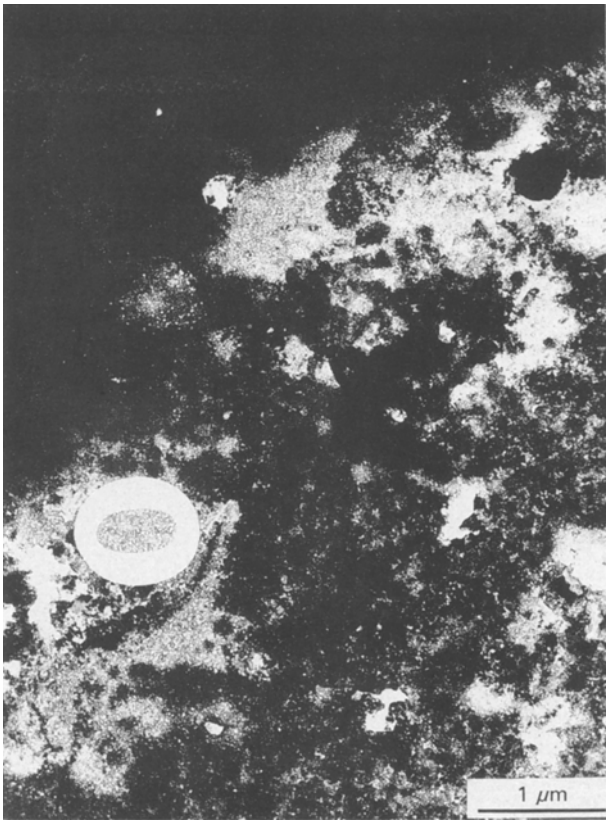

Figure 5 TEM picture around a natural hole and the selected-area diffraction pattern of the marked area of the micrograph for an ED Ni foil prepared with $i_{dep} = 500$ mA cm^{-2} and having a thickness of 5 μm (same sample as Fig. 4b). The diffraction pattern indicates the presence of amorphous NI.

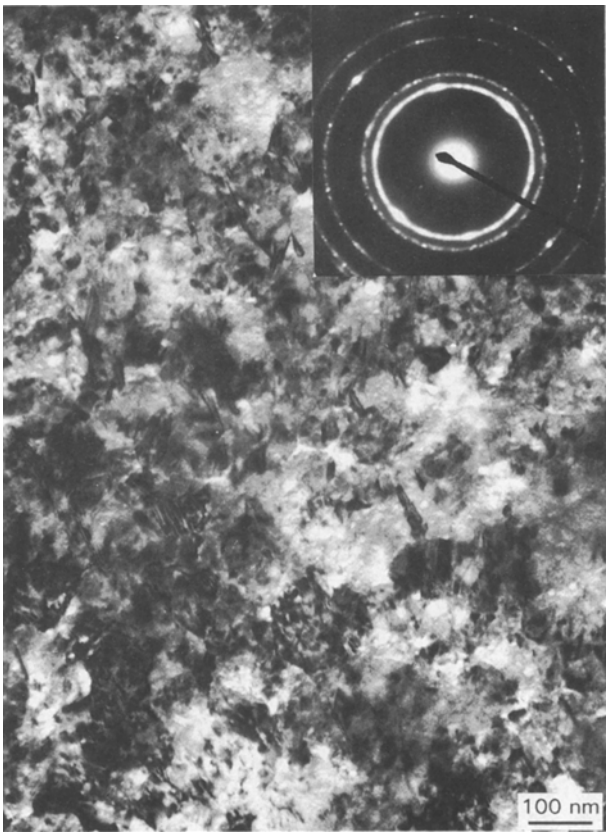

Figure 6 TEM picture and the corresponding selected-area diffraction pattern taken at higher magnification on an area exhibiting nanocrystalline structure near to the edge of the natural hole shown in Fig. 5.

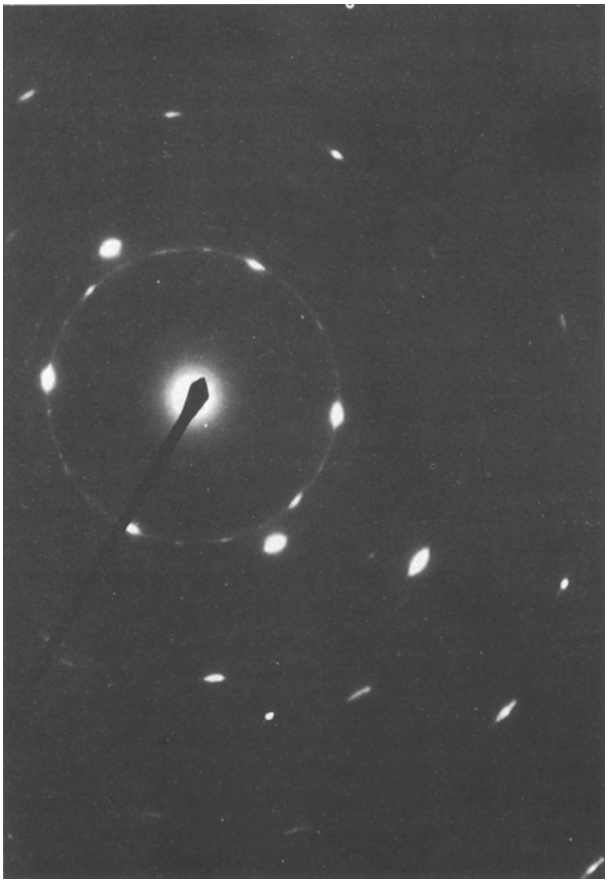

Figure 7 Selected-area diffraction pattern taken on a thicker area of the ED Ni foil of Fig. 5.

that on the thinned layers, occasionally where the thinning was effective only from one side, this kind of amorphous layer could also be detected.

In conclusion, the deposition process of pure Ni is believed to start with a very thin amorphous layer nucleated on the substrate, which is then followed by a very fine-grained nanocrystalline structure. Growing further, the crystallites become larger depending on the thickness of the sample (Fig. 8). This variation in structure across the thickness of the deposited layer can be explained reasonably well with the following considerations.

Deposition of Ni atoms starts on a pure Cu surface and is then followed by the deposition of Ni atoms on a Cu substrate, covered partially by the primarily formed islands of Ni atoms. At last, the deposition of Ni atoms proceeds on a surface fully covered by an Ni layer. This means that the electrochemical state of the substrate–and so the deposition conditions–change remarkably during the early stage of nucleation and growth of the electrodeposited Ni layers. This variation in the deposition conditions with increasing effective deposit thickness may, in turn, be accompanied by the incorporation of a similarly varying amount of (non-metallic) impurities (e.g. C) in the deposit. Although such impurities were found in only a very small amount when measured for the whole deposit thickness, their concentration could be significantly higher in a very thin surface layer of the deposit on the substrate side and then level off to a small value at larger thicknesses, due to changes of the electrochemical conditions during layer growth. Such depletion of a non-metallic component in Ni during the course of electrodeposition has, indeed, been observed [21] for the Ni–P system and may well apply also for our conditions with C as the non-metallic component.

This phenomenon would be consistent with our observations concerning the layer growth process, and also with the results of previous studies of the microstructure of thin Ni films prepared by sputtering or evaporation. Namely, as pointed out by Wright [22,23], amorphous Ni films could be obtained by these techniques only, even in the case of condensation on to a substrate at liquid helium temperature, if a small amount of impurities (preferably non-metallic) were present in the films. Thus a relatively high amount of, say, C incorporated into the ED Ni foils during the early stages of deposition could stabilize an amorphous structure as observed, whereas a gradual decrease of the amount of built-in C would result in a transition to a fine-grained, nanocrystalline structure first and, finally, a low concentration of C at even

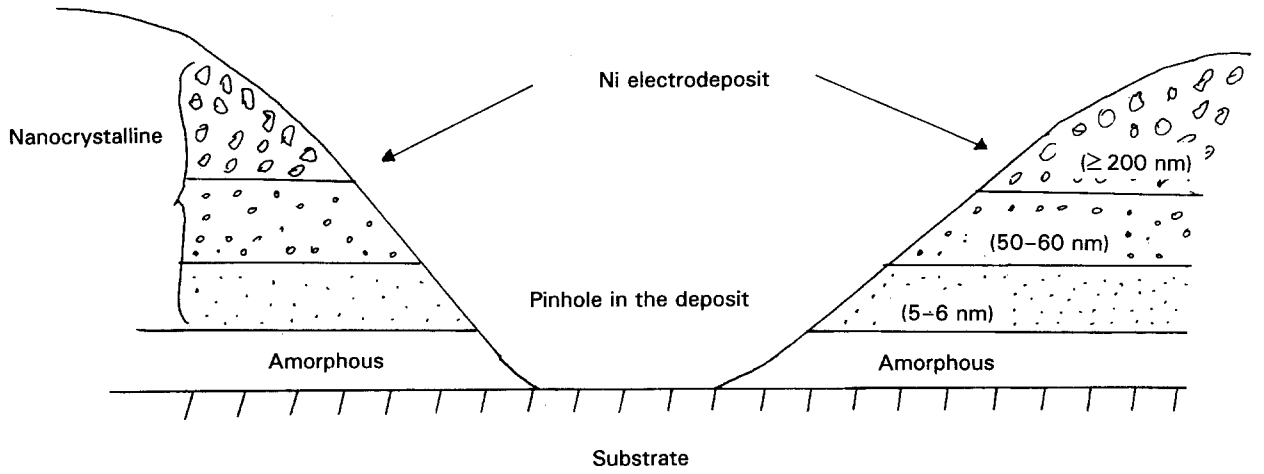

Figure 8 Sequence of different structure types as formed in the ED Ni foils during the deposition process (schematic picture of the neighbourhood of a pinhole). The numbers in parentheses indicate the average grain sizes.

higher thicknesses could no longer prevent the formation of relatively large grains.

Another factor which may have an influence on the microstructure of ED Ni foils [12,24] is the presence of atomic hydrogen at the cathode surface. Since the amount of hydrogen present at the cathode surface and/or incorporated into the deposit can be assumed to vary substantially with the deposition current density, this may partly explain our observation of a change of grain size with i_{dep}; this phenomenon, however, requires further studies.

4. Summary

It has been found that both the deposition current density and the deposit thickness can strongly affect the microstructure of electrodeposited Ni foils. The observed variation of the grain size correlates with the magnitude of the electrical resistivity and its temperature coefficient for these ED Ni samples. On the basis of the detected structure of the ED Ni samples, a model has been suggested for the growth of the foils which involves a gradual coarsening of the grain size during deposition.

Acknowledgements

This work was supported by the OTKA Board of Hungary through grant No. 2942. The copper substrate foils were kindly donated by the Csepel Metal Works, Budapest.

References

1. H. GLEITER, *Progr. Mater. Sci.* **33** (1989) 223.
2. K. L. MERKLE and D. J. SMITH, *Phys. Rev. Lett.* **59** (1987) 2887.
3. G. WALLNER, E. JORRA, H. FRANZ, J. PEISL, R. BIRRINGER, H. GLEITER, T. HAUBOLD and W. PETRY, *Mater. Res. Soc. Symp. Proc.* **132** (1989) 149.
4. E. JORRA, H. FRANZ, J. PEISL, G. WALLNER, W. PETRY, R. BIRRINGER, H. GLEITER and T. HAUBOLD, *Philos. Mag. B* **60** (1989) 159.
5. X. ZHU, R. BIRRINGER, U. HERR and H. GLEITER, *Phys. Rev. B* **35** (1987) 9085.
6. T. HAUBOLD, R. BIRRINGER, R. LENGELER and H. GLEITER *J. Less-Common Metals.* **145** (1988) 557.
7. G. J. THOMAS, R. W. SIEGEL and J. A. EASTMAN, *Scripta Metall. Mater.* **24** (1990) 201.
8. M. R. FITZSIMMONS, J. A. EASTMAN, M. MÜLLER-STACH and G. WALLNER, *Phys. Rev. B* **44** (1991) 2452.
9. J. A. EASTMAN, M. R. FITZSIMMONS, M. MÜLLER-STACH, G. WALLNER and W. T. ELAM, *Nanostruct. Mater.* **1** (1992) 47.
10. J. A. EASTMAN, M. R. FITZSIMMONS and L. J. THOMPSON, *Phil. Mag. B* **66** (1992) 667.
11. H. MAEDA, *Jpn. J. Appl. Phys.* **8** (1969) 978.
12. S. KAJA, H. W. PICKERING and W. R. BITLER, *Plat. Surf. Fin.* **73** (1) (1986) 58.
13. G. PALUMBO, D. M. DOYLE, A. M. EL-SHERIK, U. ERB and K. T. AUST, *Scripta Metall. Mater.* **25** (1991) 679.
14. I. BAKONYI, E. TÓTH-KÁDÁR, T. TARNÓCZI, L. K. VARGA, Á. CZIRÁKI, I. GERÖCS and B. FOGARASSY, *Nanostruct. Mater.* **3**, (1994) 155.
15. E. TÓTH-KÁDÁR, I. BAKONYI, A. SÓLYOM, J. HERING, G. KONCZOS and F. PAVLYÁK, *Surf. Coat. Technol.* **31** (1987) 31.
16. E. TÓTH-KÁDÁR, Hungarian Patent 195 982 (1984).
17. M. J. LAUBITZ, T. MATSUMURA and P. J. KELLY, *Can. J. Phys.* **54** (1976) 92.
18. I. A. CAMPBELL and A. FERT, in "Ferromagnetic Materials", Vol. 3, edited by E. P. Wohlfarth (North-Holland, Amsterdam, 1982) p. 747.
19. M. C. CADEVILLE and C. LERNER, *Phil. Mag.* **33** (1976) 801.
20. J. H. MOOIJ, *Phys. Status Solidi (a)* **17** (1973) 521.
21. U. PITTERMANN and S. RIPPER, in "Rapidly Quenched Metals", edited by S. Steeb and H. Warlimont (North-Holland, Amsterdam, 1985) p. 385.
22. J. G. WRIGHT, *IEEE Trans. Magn.* **MAG-12** (1976) 95.
23. *Idem, Inst. Phys. Conf. Series* No. 30 (1977) 251.
24. S. NAKAHARA and E. C. FELDER, *J. Electrochem. Soc.* **129** (1882) 45.

Received 11 May 1993
and accepted 21 March 1994